Science & Technology Development Journal – Engineering and Technology, 4(4):1219-1228

Open Access Full Text Article

Research article

Settling behaviour of irregular-shaped polystyrene microplastics

Thu Ha Nguyen*

Use your smartphone to scan this QR code and download this article

ABSTRACT

Microplastics are emerging pollutants that can pose threats to aquatic ecosystems by carrying toxic additives to the food web. Their abundance has been reported in many waterways globally, including the Sai Gon River, Vietnam. A good understanding of microplastic sinking behaviours can help predict the distribution and removal of these pollutants in water. Microplastic dynamics are still mostly assumed to be similar to that of suspended sediment. However, MPs possess many artificial properties that can make them move distinctly in the water from suspended sediment like densities, structures, shapes, and surface properties. This research, therefore, aims to investigate the correlation of the polystyrene microplastic size and irregular shapes with its vertical movement. The experiments employed the Particle Tracking Velocimetry (PTV) method and an automatic image processing algorithm to simultaneously measure MP geometrical properties and settling velocity while freely settling in a still water column. We found that the circumscribed diameter is the most appropriate geometrical parameter to represent MP size. The settling velocity of irregular-shaped polystyrene microplastics in size of 0.2 to 0.9 mm is mostly between 0.5 and 2 mm/s, half of the sediment but four-fold that of biological aggregates at the same size. The settling velocity increases two-fold when MP size enlarges from 0.2 to 0.9 mm. The shape irregularity can slow down the sinking of large microplastics but do not affect the vertical movement of microplastics smaller than 0.32 mm. The ratio between microplastic projected area and the area of the smallest circumscribed circle was found to be the two-dimensional representation of three-dimensional shapes in the correlation between size and settling velocity. Therefore, the fitting curve equations suggested herein can be used as a simple tool to estimate the settling velocity of irregular-shaped polystyrene microplastics found in many in-situ sampling campaigns.

Key words: microplastics, settling velocity, irregularity, shape factors, polystyrene

Faculty of Civil Engineering, Ho Chi Minh City University of Technology, VNU-HCM, Ho Chi Minh City, Vietnam

Correspondence

Thu Ha Nguyen, Faculty of Civil Engineering, Ho Chi Minh City University of Technology, VNU-HCM, Ho Chi Minh City, Vietnam

Email: thuhatnn@hcmut.edu.vn

History

- Received: 14-8-2021
- Accepted: 27-11-2021
- Published: 25-12-2021

DOI : 10.32508/stdjet.v4i4.879

VNU-HCM Press

INTRODUCTION

The growing human population with the consequences of industrial development has irreversibly changed natural water conditions. Since the Industrial Revolution, new materials have been invented and massively used as replacements for traditional materials. One of the revolutionary innovations is plastic, which possesses many advantages, including resistance to corrosion, lightweight, high strength, transparency, durability, low costs, and convenience in use[1]. Plastic has been used in almost every corner of the globe, from industry to daily life, with global plastic production has reached 368 million tonnes in 2019[2]. However, plastic production and use have not been accompanied by efficient plastic waste management; consequently, natural waters have become a plastic discharge destination receiving 2.41 million tonnes of plastic waste annually[3,4]. Plastics in natural waters not only act as deadly traps to aquatic organisms and fish-eating birds but also can be degraded into smaller pieces (< 5mm), namely microplastics (MPs), which are widely known to be able to bioaccumulate and carry harmful chemicals throughout the food web[5,6]. The hydrodynamic properties of MP pollutants determine whether they would spread throughout the water column, to offshore waters, or are buried in bed sediment but are still not well-studied.

Although MPs are also suspended particles like mineral sediment, MPs possess many artificial properties that can make them move distinctly in the water from suspended sediment. Firstly, MPs are made of various polymers with density ranging from 11 kg/m^3 of expanded polystyrene, 880 kg/m^3 of polyethylene, 1050 kg/m^3 of polystyrene (PS) to 1380 kg/m^3 of polyethylene terephthalate as compared to mineral sediment density of 2650 kg/m^3 [7]. Therefore, a polystyrene MP sphere needs to be eight times larger in size to sink at the same speed as a sediment aggregate[8,9]. Secondly, while sediment mainly exists as aggregates of multi-particles with fractal dimensions smaller than 3, MPs are dense particles with fractal dimensions equal to 3. However, MPs are highly variable in shapes, typically one-dimensional (fibres, lines), two-dimensional (films, flakes), and three-dimensional

Cite this article : Nguyen T H. **Settling behaviour of irregular-shaped polystyrene microplastics**. *Sci. Tech. Dev. J. – Engineering and Technology;* 4(4):1219-1228.

(pellets, fragments). Experiments of settling velocity of MPs showed that the fragment and regular-shape MPs sink and rise faster than the line ones [10,11]. The effect of shapes on velocities can even dominate that of densities [12]. Thirdly, MPs are added additives during plastic production that causes MPs surface properties to be different from natural minerals, such as MPs have higher hydrophobicity than minerals [8]. Highly hydrophobic particles were shown to be subjected to lower drag force and thus settle at a higher speed than those with low hydrophobicity [13]. Therefore, the extensive knowledge of sediment hydrodynamics could not be straightforwardly applied to MPs but required more experimental evidence to connect this knowledge to MPs.

Most MPs are the degradations of macro and mesoplastics due to weathering and external forces, thus mostly being found in irregular shapes [14]. The common knowledge is that particles with shapes further from the sphere would have higher drag coefficients and lower settling velocity [15,16]. Although some experiments have established the correlation between MP shapes and settling velocity [8,15,17], the shape factors used in these studies require a three-dimensional (3D) size of the particles (e.g., length, width, and thickness), which are hard to retrieve from a two-dimensional (2D) device like microscopes. In fact, most of the MP sampling campaigns nowadays provide 2D microscopic images of real MPs from natural water bodies [14,18]. The geometrical properties of MPs retrieved from these images could be helpful to predict MP transport if a correlation between MP settling velocity and 2D shape properties are established.

This paper aims to examine (i) the settling velocity of irregular shaped polystyrene MPs in size of 150 – 900 μm, (ii) the correlation between shapes and settling velocity for these MPs, and (iii) whether 2D shape factors can represent MP shapes in the correlations. We conducted the experiment using the particle tracking velocimetry (PTV) method, and an automatic image processing algorithm was employed to simultaneously retrieve MP sizes, shapes, and settling velocities.

MATERIALS AND METHODS

Materials

Microplastics used in this experiment is commercial polystyrene (PS) particles with an average manufactured size of 150 μm. PS is a popular polymer to make single-use plastics such as take away food packaging and labware. PS particles in this experiment are black and white 3D irregular-shaped with a density of 1050 kg/m^3. PS particles were stirred and submerged in tap water before the experiment.

Settling velocity measurement

The settling test was conducted in a 25x25x50 cm acrylic settling column filled with tap water at room temperature at about 30°C (Figure 1). A 7 mm sampling hole was prepared at the column cap, where a 5-cm-long straw was put in place to guide the movement of MPs to the camera field of view. The camera was positioned opposite the cool white 220 V - 3 Watt LED light source and about 20 cm from the sampling hole. MPs were transferred to the settling column using a wide mouth pipette inserted into the sampling hole. When MPs were freely settling to the camera field of view, their shadow images were acquired by the camera. Two images were captured per acquisition for the settling velocity calculation. The image acquisition only occurred after the pipette was inserted into the sampling hole for 10 seconds to minimise the interference of manual sampling. The optic setting includes a Canon EOS M6 Mark II camera paired with a Canon MP-E65mm f2.8 1-5X lens at a resolution of 1.08 μm/pixel and the field of view 7.5x6.0 mm.

Image processing algorithm

The image processing algorithm analysed only the blue pixel intensity B_p of the full-colour raw images from the settling test (detailed in Figure 2). B_p was then subtracted by the background blue intensity B_{BG}, which was acquired before inserting MPs. After the subtraction, B_p of MPs is higher than the background B_p, and then an intensity threshold was set to filter background pixels. Individual MP images were extracted from the full-field-of-view images following an image recognition algorithm [19] and then tested for focus levels, which are best described for this dataset by the grey level local variance (Pech-Pacheco et al., 2000) and histogram entropy [20] methods. By that means, an in-focus MP image would have high-intensity gradient (i.e., variance > 100000) and sharp edges (i.e., edge intensity histogram entropy < 6.9). In-focus MP images were then analysed to retrieve geometrical properties such as length, width, circumscribed and inscribed circle diameters, area, perimeter and shape factors. Because more than one MP may be captured in the field of view in one shot, an MP particle from two sequential frames were recognised if their size, area matched more than 90% and their diagonal travel distance smaller than the field of view size [21]. The settling velocity v was finally calculated as the ratio of the MP vertical distance Δy and the gap time Δt between the two continuous frames (Eq. 1).

$$v = \frac{\triangle y}{\triangle t} \quad (1)$$

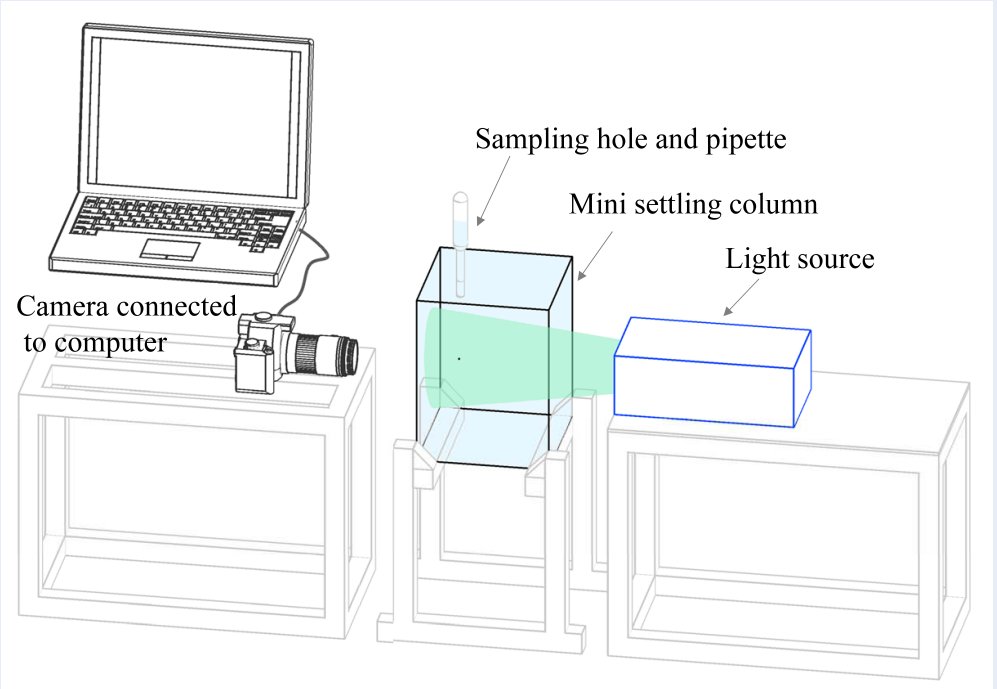

Figure 1: Conceptual representation of the experimental setup.

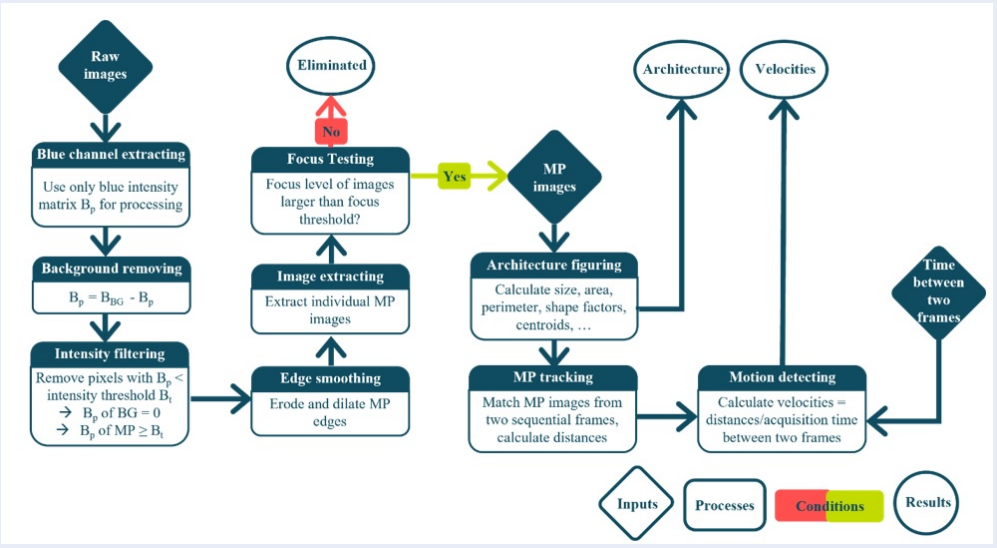

Figure 2: Image processing algorithm.

Shape analyses

Many shape measures have been introduced to characterise non-spherical particles, such as the volume-equivalent-sphere diameter, sphericity[22], and Corey shape factor CSF[23]. In this analysis, we mainly focused on 2D shape factors. Because the MPs used in our experiment are 3D (i.e., the differences in three dimensions are less than one order of magnitude), we assume that the projections of each MP particle are similar in all directions.

One of the 2D shape measures is the projected area diameter D_A[24], which is the diameter of a sphere having the same projected area as the MP particle, as below

$$D_A = \sqrt{4A_{MP}/\pi} \quad (2)$$

where A_{MP} is the projected area of the MP particle. Three dimensionless shape factors were considered that involved different MP geometrical properties. The projection sphericity ψ[25] compares the circumscribed and inscribed circles of an MP particle as

$$\psi = \sqrt{D_o/D_i} \quad (3)$$

where D_o and D_i are the diameters of the smallest circumscribed circle and the largest inscribed circle of the MP, respectively. The circularity c[22] is the ratio between the perimeters of the projected-area-equivalent-sphere and the MP particle P_{MP}.

$$c = \frac{\pi D_A}{P_{MP}} = \frac{\sqrt{\pi A_{MP}}}{P_{MP}} \quad (4)$$

Microplastic 2D shapes can also be analysed as a ratio between the projected area A_{MP} and the area of the smallest circumscribed circle A_o, called operational circularity c_o[22].

$$c_o = \frac{A_{MP}}{A_o} = \frac{4A_{MP}}{\pi D_o^2} \quad (5)$$

These three shape factors equal 1 for a sphere or a particle with a round projection area and less than one for other shapes.

The goodness of fit of observed data o and fitted curves e was quantified throughout the analyses by the correlation coefficient $R = cov(e,o)/(\sigma_e\sigma_o)$ and the percentage error $PE = \sum_{k=1}^{n}|e_k - o_k| / \sum_{k=1}^{n} o_k \times 100\%$, where σ_e and σ_o were the standard deviation of e and o, respectively. One-way analysis of variance ANOVA was used to test the correlation between pairs of parameters described above with the null hypothesis that one variable is invariant across the range of the other parameter. The null hypothesis is rejected if $p < 0.001$, which means the tested correlation is significant.

RESULTS

MP sizes and shapes

522 pairs of MP particle images retrieved from the experiment were used for the analyses. Their diameters of circumscribed D_o and inscribed D_i circles were shown in Figure 3, corresponding to the projection sphericity ψ. D_i ranged around the MPs manufactured size (i.e., 150 μm) while D_o can be six times larger than that size. Therefore, D_i and D_o can be a proxy for the thickness and length of MP particles. The broad range of D_o can be referred to as the elongated shapes or the aggregation of MP particles (see examples of MP images in Figure 3). MPs with D_o larger than 400 μm are more likely to be aggregates of two or more MP particles. Unlike dense MP particles, the aggregates of MPs can have holes in between, making the shapes more complicated. Some MPs have a very rough surface reflected by the variable image intensity. Most MP shapes in this experiment are far from a sphere ($\psi = 1$), with the highest and lowest sphericity of 0.92 and 0.42, respectively. At the same D_i, MPs with higher D_o would have lower ψ and vice versa; at the same D_o, MPs with higher D_i would have higher ψ.

MP sizes and settling velocity

Figure 4 depicts the response of settling velocity v to MP sizes, which are reported herein as MP projected area diameter D_A and circumscribed circle diameter D_o. In general, v increases almost double with increasing size from 173 to 495 μm for D_A and from 202 to 902 μm for D_o, and these relationships are significant ($p < 0.001$) in the ANOVA tests. However, the data is highly scattered; the standard deviation of bin averaged v for different size range varies from $\pm$0.3 to $\pm$0.6 mm/s for D_A and $\pm$0.3 to $\pm$1 mm/s for D_o. Highly scattered data is likely because more factors control MP settling velocity rather than MP size, like MP shapes. Another reason for this scatteredness is the use of 2D images for irregular shape MPs. As in the previous section, MPs thickness and length (D_i and D_o) are not similar, and thus one MP captured in different views can have different sizes and shapes. This is, however, the method intrinsic nature, and thus the bin-averaged values and the trend of fitting lines is still statistically reliable due to the high number of samples.

The range of D_A is narrower than the D_o range. Therefore, the fitting curve of bin-averaged $\bar{v}$ versus D_A is slightly steeper than that of D_o. The goodness of fit

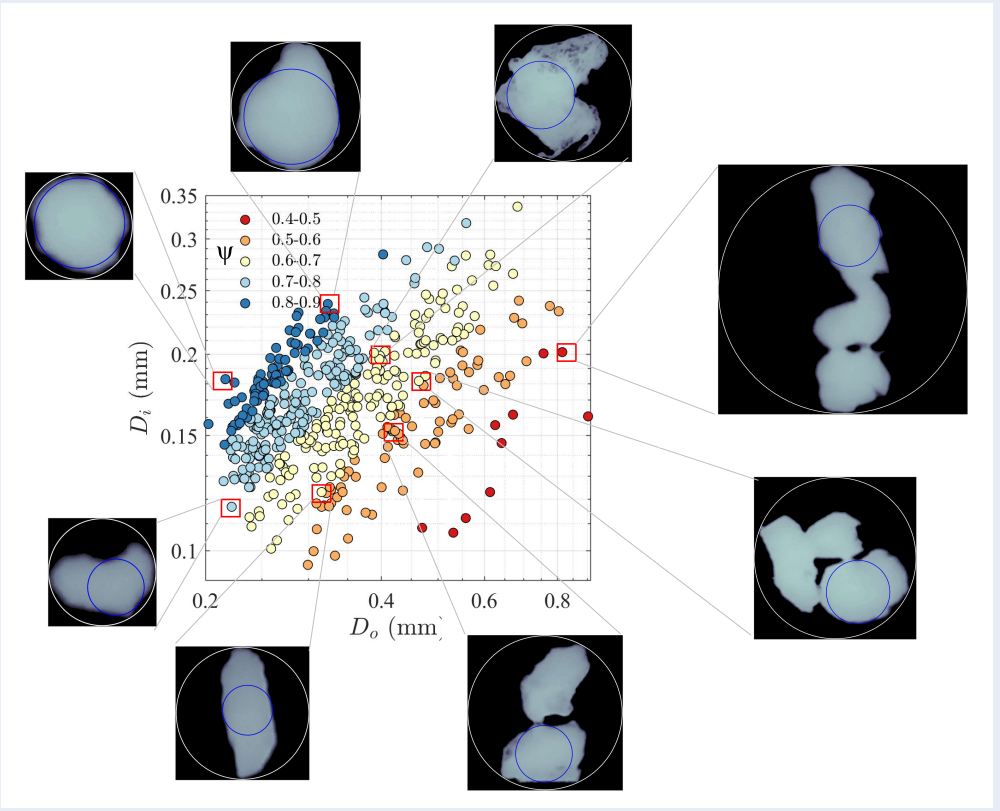

Figure 3: Diameters of MP circumscribed (D_o) and inscribed (D_i) circles, at ranges of projection sphericity ψ. Example images of MP at various combination of D_o and D_i with white and blue circles being circumscribed and inscribed circles, respectively.

for $\bar{v}$ versus D_A is R = 0.92, PE = 6.44% and for $\bar{v}$ versus Do is R = 0.96, PE = 4.17%. Moreover, we recognised that Do has a better correlation with shape factors than D_A, and the wide range of Do give a more graphic description of MP size than D_A. As a result, Do is chosen to represent MP size for further analysis.

MP shapes and settling velocity

Although all three shape factors, projection sphericity ψ, circularity c, and operational circularity c_o, have the same maximum value of 1 when a particle has a circular projection, their probability distribution for the same data set is largely distinct (Figure 5 a). The values of c are the highest, with the majority being higher than 0.8, followed by ψ (i.e., mostly 0.6 to 0.85) and c_o. The range of c_o is the widest, i.e., 0.2 to 0.82, and thus may better represent the irregularity of MP shapes.

The values of ψ, c, c_o were plotted against v in Figure 5b to test the effects of shape factors on settling velocity. Contrary to common sense that a higher degree of irregular shape would dramatically hinder the MP settling, higher v was observed at smaller ψ, c, c_o. This correlation, though, is only significant ($p < 0.001$) for ψ. It can be inferred that although a highly irregular shape could enlarge the surface area leading to a higher drag force on MPs than a sphere, decreasing shape factors also accords with increasing size (Figure 5c). The effect of size on v may overcome that of shape factors on v, thus causing v to increase when MP shapes become more irregular.

To minimise the effect of size on the analysis of shape factors and settling velocity, we took the bin-average of v for different ranges of D_o and ψ, c, c_o (Figure 6). At the same size, the settling velocity of smaller ψ, c, c_o, i.e., more irregular, is lower than that of higher ψ, c, c_o. Then the ANOVA tests were conducted for the correlation of $\bar{v}$ and ψ, c, c_o at 3 ranges of D_o (Table 1). The null hypothesis was rejected for the correlation of $\bar{v}$ and c_o for $D_o > 0.32$ mm and mostly accepted for that of ψ and c. Therefore, c_o was shown to be the most appropriate 2D factor to represent MP shapes. More importantly, we can conclude that the shape irregularity can slow down the sinking of large MPs but

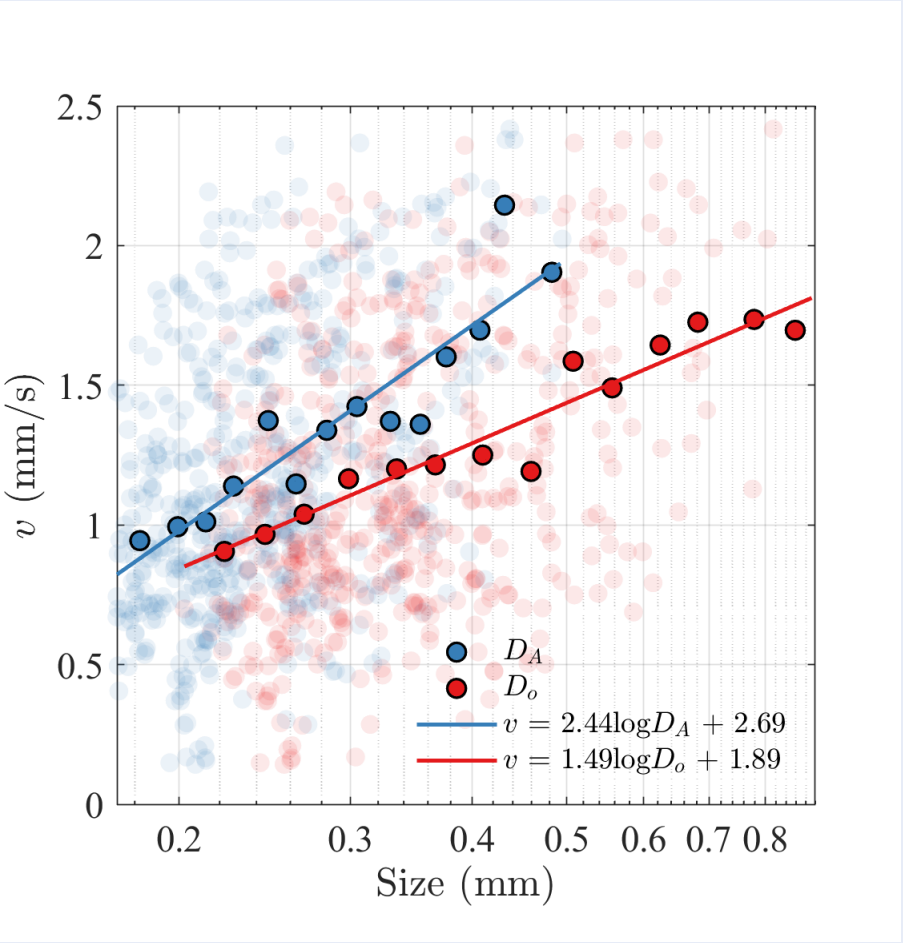

Figure 4: Settling velocity v as functions of MP size. D_A (blue) is projected area diameter and D_o (red) is MP circumscribed circle diameter. Scattered points are observed data, black-edge-circles are bin-averaged data, and lines are fitting curves. Symbol " – " means the null hypothesis in the ANOVA tests were rejected for the corresponding data.

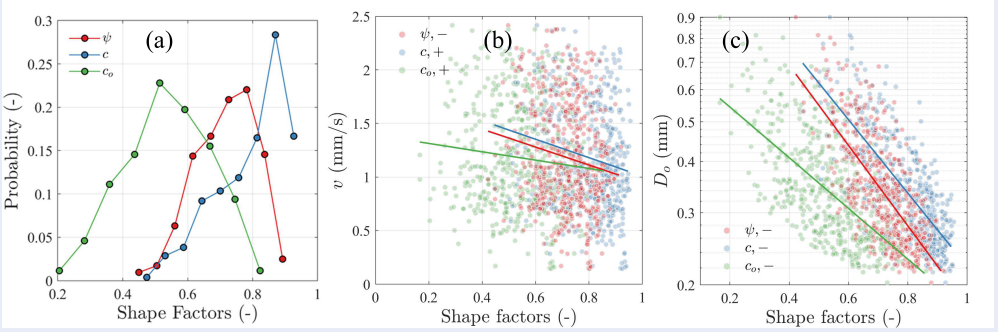

Figure 5: Shape factors analyses. (a) Probability of observing the shape factors: projection sphericity ψ, circularity c, and operational circularity c_o; (b) settling velocity versus ψ, c, c_o; (c) MP circumscribed circle diameter D_o versus ψ, c, c_o. The lines in (b, c) are trend lines; symbols " – " and " + " mean the null hypothesis in ANOVA tests were rejected and accepted for the corresponding data.

have no effect on the vertical movement of small MPs (e.g., D_o < 0.32 mm).

Table 1: ANOVA results for shape factors and settling velocity correlation at different MP size. Symbols " – " and " + " mean the null hypothesis were rejected (p > 0.001) and accepted (p > 0.001), respectively.

	D_o (mm)			
	0.20 – 0.32	–	0.32 – 0.46	0.46 – 0.90
v – ψ	+		+	-
v – c	+		+	+
v – c_o	+		-	-

MP size, shapes and settling velocity

The correlation between MP size D_o and settling velocity v were analysed at four ranges of shape factors ψ, c, c_o (Figure 6). These ranges were set as evenly spaced intervals of the whole data of ψ, c, c_o. Significant relationships between $\bar{v}$ and D_o were found at c_o > 0.34 and fewer ranges of ψ, c. Insignificant $\bar{v}$ and D_o correlation at c_o < 0.34 suggests that when the irregularity level is too high, the MP settling regime will not be dominantly controlled by size. The averaged values of v can, therefore, be predicted using the fitting curves (Eqs. 6) if an MP circumscribed circle diameter D_o and operational circularity (c_o > 0.34) were given.

$$v = 2.44 \log D_o + 2.23, \; if \; 0.34 \leq c_o < 0.51 \quad (6a)$$

$$v = 1.58 \log D_o + 2.01, \; if \; 0.51 \leq c_o < 0.69 \quad (6b)$$

$$v = 2.80 \log D_o + 2.70, \; if \; 0.69 \leq c_o < 0.86 \quad (6c)$$

The goodness of fit of Eqs. 6 are 0.86 < R < 0.93 and 5.4% < PE < 10%.

DISCUSSION

The polystyrene MP size used in this experiment is different from those studied in other experiments (e.g., 0.2 to 0.9 mm herein smaller than 1.25 – 2.13 mm in [8], 1.6 – 1.8 mm in [12], and larger than 0.007 to 0.03 mm in [26]). Therefore, this paper has filled the gap for the settling velocity data for particles from 0.1 to 1 mm, which has been found abundant in riverine ecosystems [27]. As a result, the settling velocity values in our experiment are in between the velocity ranges of previous experiments. [12] reported a control set of 0.5 mm PS spheres that has v about 5.6 mm/s, more than double v in this experiment. This difference is likely because of the effect of shapes with spheres (c_o = 1) settling faster than the irregular shapes (c_o <0.86) herein.

In natural water environments like rivers and oceans, suspended particular matter size 0.2 - 0.9 mm as MPs in this experiment includes biological aggregates (e.g., cell clusters or cells and organic matter with density $\rho \approx 1050$ kg/m^3), biomineral aggregates (e.g., aggregates of suspended sediment minerals and organic matter at various material fractions with $\rho \approx 1400$ – 2400 kg/m^3), mineral aggregates (e.g., mud, clay aggregates or combination of different mineral types with $\rho \approx 2650$ kg/m^3), and MPs of other polymers (e.g., $\rho \approx 11$ – 1380 kg/m^3) [7,9]. Unlike dense MPs, other suspended materials at this size range are aggregates with fractal dimensions smaller than 2.2 [9]. Thus the settling velocity of different materials cannot be compared only by size, densities, or shapes but also by aggregate structures. For example, although biological aggregates have similar density and size with polystyrene, their settling velocity is only one-fourth of PS particles in this experiment. On the other hand, equal-size mineral aggregates settle two-fold as fast as the MPs herein. At the same size, polystyrene MPs can settle at the same speed as biomineral aggregates with 82% cell fraction [9] and polyurethane MPs colonised by cells up to 60% [28].

Depending on the analyses' samples, materials, and purposes, previous research has suggested various shape factors to illustrate suspended particle shapes. For example, [8] recommended using circularity c to differentiate fibrous and non-fibrous MPs while using sphericity to classify film and non-film MPs. [16] found the coupling of D_A/D_n and circularity c to be the best shape factors to formalise the shapes and settling velocity correlation of non-spherical particles in general, where D_n is the volume-equivalent-sphere diameter. In this research, the operation circularity c_o has been proved to be the most appropriate 2D shape factor to represent the irregularity of a 3D microplastic particle in the correlation between settling velocity and size.

CONCLUSION

This research experimentally established the correlation between polystyrene microplastic sizes and 2D shapes and settling velocity using the particle tracking velocimetry (PTV) method. The irregular-shaped polystyrene was at the size range of 0.2 to 0.9 mm. The shape irregularity can slow down the sinking of large microplastics but do not affect the vertical movement of those smaller than 0.32 mm. The positive correlation between settling velocity and size also becomes

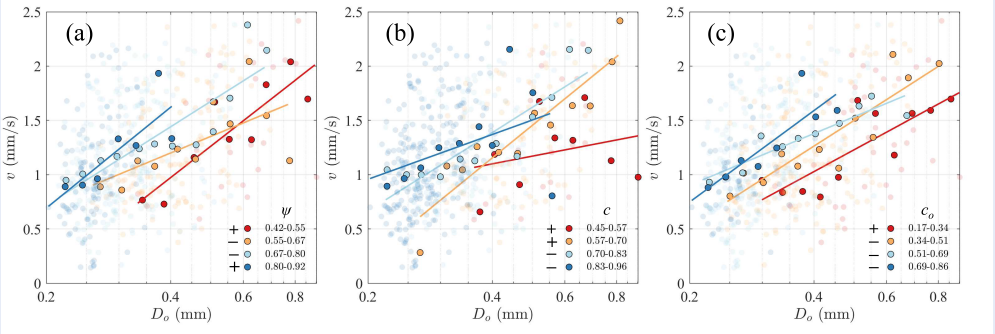

Figure 6: MP settling velocity versus size at different ranges of shape factors; (a) projection sphericity ψ, (b) circularity c, and (c) operational circularity c_o. Scattered points are observed data, black-edge-circles are bin-averaged data, and lines are fitting curves; symbols " – " and " + " mean the null hypothesis in ANOVA tests were rejected and accepted for v at ranges of D_o for corresponding shape factor values.

insignificant when the level of irregularity is too high. The operational circularity c_o, the ratio between microplastic projected area and the area of the smallest circumscribed circle, was found to be the 2D representation of 3D shapes in the correlation between settling velocity and size. Therefore, the fitting curve equations between settling velocity and size at different c_o values suggested herein can be used as a simple tool to estimate the settling velocity of irregular-shaped polystyrene microplastics found in many in-situ sampling campaigns.

LIST OF ABBREVIATIONS

MPs: Microplastics
PS: Polystyrene
PTV: Particle tracking velocimetry

COMPETING OF INTERESTS

The author declares that there are no competing interests.

AUTHOR CONTRIBUTION

Thu Ha Nguyen conceptualised the research and methodology, set up and conducted the experiments, processed images, analysed data, wrote and revised the manuscript.

ACKNOWLEDGEMENTS

This research is funded by Ho Chi Minh City University of Technology (VNU-HCM), under grant number T-KTXD-2020-76, and the experimental facilities are supported by the project JEAI PLASTIC of the French National Research Institute for Sustainable Development (IRD).

REFERENCES

1. Nature Communications Editorial. The future of plastic. Nat Commun [Internet]. 2018 Jun 5 [cited 2021 Aug 14];9(1):2157;Available from: https://doi.org/10.1038/s41467-018-04565-2.
2. PlascticsEurope. Plastics-the Facts 2020 An analysis of European plastics production, demand and waste data [Internet]. 2020 [cited 2021 Aug 14];Available from: https://www.plasticseurope.org/.
3. Lebreton LCM, der Zwet J, Damsteeg J-W, Slat B, Andrady A, Reisser J. River plastic emissions to the world's oceans. Nat Commun [Internet]. 2017 [cited 2021 Aug 14];8:15611;PMID: 28589961. Available from: https://doi.org/10.1038/ncomms15611.
4. Jambeck JR, Geyer R, Wilcox C, Siegler TR, Perryman M, Andrady A, et al. Plastic waste inputs from land into the ocean. Science [Internet]. 2015 [cited 2021 Aug 14];347(6223):768-71;PMID: 25678662. Available from: https://doi.org/10.1126/science.1260352.
5. Andrady AL. Microplastics in the marine environment. Mar Pollut Bull [Internet]. 2011 [cited 2021 Aug 14];62(8):1596-605;Available from: https://doi.org/10.1016/j.marpolbul.2011.05.030.
6. Rochman CM, Browne MA, Underwood AJ, van Franeker JA, Thompson RC, Amaral-Zettler LA. The ecological impacts of marine debris: Unraveling the demonstrated evidence from what is perceived. Ecology [Internet]. 2016 [cited 2021 Aug 14];97(2):302-12;Available from: https://doi.org/10.1890/14-2070.1.
7. Chubarenko I, Esiukova E, Bagaev A, Isachenko I, Demchenko N, Zobkov M, et al. Behavior of microplastics in coastal zones. In: Microplastic contamination in aquatic environments [Internet]. Elsevier; 2018 [cited 2021 Aug 14]. p. 175-223;Available from: https://doi.org/10.1016/B978-0-12-813747-5.00006-0.
8. Melkebeke M, Janssen C, de Meester S. Characteristics and Sinking Behavior of Typical Microplastics Including the Potential Effect of Biofouling: Implications for Remediation. Environmental Science & Technology [Internet]. 2020 Jul 21 [cited 2021 Aug 14];54(14);Available from: https://doi.org/10.1021/acs.est.9b07378.
9. Maggi F, Tang FHM. Analysis of the effect of organic matter content on the architecture and sinking of sediment aggregates. Mar Geol [Internet]. 2015 [cited 2021 Aug 14];363:102-11;Available from: https://doi.org/10.1016/j.margeo.2015.01.017.
10. Kooi M, Reisser J, Slat B, Ferrari FF, Schmid MS, Cunsolo S, et al. The effect of particle properties on the depth profile of

buoyant plastics in the ocean. Sci Rep [Internet]. 2016 [cited 2021 Aug 14];6:33882;Available from: https://doi.org/10.1038/srep33882.
11. Khatmullina L, Isachenko I. Settling velocity of microplastic particles of regular shapes. Mar Pollut Bull [Internet]. 2017 [cited 2021 Aug 14];114(2):871-80;Available from: https://doi.org/10.1016/j.marpolbul.2016.11.024.
12. Kowalski N, Reichardt AM, Waniek JJ. Sinking rates of microplastics and potential implications of their alteration by physical, biological, and chemical factors. Mar Pollut Bull [Internet]. 2016 [cited 2021 Aug 14];109(1):310-9;Available from: https://doi.org/10.1016/j.marpolbul.2016.05.064.
13. Wang L, Zheng K, Ding Z, Yan X, Zhang H, Cao Y, et al. Drag coefficient and settling velocity of fine particles with varying surface wettability. Powder Technology [Internet]. 2020 Jul [cited 2021 Aug 14];372;Available from: https://doi.org/10.1016/j.powtec.2020.05.102.
14. Lahens L, Strady E, Kieu-Le T-C, Dris R, Boukerma K, Rinnert E, et al. Macroplastic and microplastic contamination assessment of a tropical river (Saigon River, Vietnam) transversed by a developing megacity. Environ Pollut [Internet]. 2018 [cited 2021 Aug 14];236:661-71;Available from: https://doi.org/10.1016/j.envpol.2018.02.005.
15. Waldschläger K, Schüttrumpf H. Effects of particle properties on the settling and rise velocities of microplastics in freshwater under laboratory conditions. Environmental Science & Technology [Internet]. 2019 Feb 19 [cited 2021 Aug 14];53(4);Available from: https://doi.org/10.1021/acs.est.8b06794.
16. Tran-Cong S, Gay M, Michaelides EE. Drag coefficients of irregularly shaped particles. Powder Technology [Internet]. 2004 Jan [cited 2021 Aug 14];139(1);Available from: https://doi.org/10.1016/j.powtec.2003.10.002.
17. Kaiser D, Estelmann A, Kowalski N, Glockzin M, Waniek JJ. Sinking velocity of sub-millimeter microplastic. Marine Pollution Bulletin [Internet]. 2019 Feb [cited 2021 Aug 14];139;Available from: https://doi.org/10.1016/j.marpolbul.2018.12.035.
18. Strady E, Kieu-Le T-C, Gasperi J, Tassin B. Temporal dynamic of anthropogenic fibers in a tropical river-estuarine system. Environmental Pollution [Internet]. 2020 Apr [cited 2021 Aug 14];259;Available from: https://doi.org/10.1016/j.envpol.2019.113897.
19. Maggi F. Variable fractal dimension: A major control for floc structure and flocculation kinematics of suspended cohesive sediment. J Geophys Res Oceans [Internet]. 2007 [cited 2021 Aug 14];112(C7);Available from: https://doi.org/10.1029/2006JC003951.
20. Krotkov E. Focusing. International Journal of Computer Vision [Internet]. 1987 [cited 2021 Aug 14];1:223-37;Available from: https://doi.org/10.1007/BF00127822.
21. Tang FHM, Maggi F. A mesocosm experiment of suspended particulate matter dynamics in nutrient-and biomass-affected waters. Water Res [Internet]. 2016 [cited 2021 Aug 14];89:76-86;Available from: https://doi.org/10.1016/j.watres.2015.11.033.
22. Wadell H. Sphericity and roundness of rock particles. The Journal of Geology [Internet]. 1933 Apr [cited 2021 Aug 14];41(3):310-31;Available from: https://www.jstor.org/stable/30058841.
23. Corey AT. Influence of shape on the fall velocity of sand grains [Internet]. [Colorado]; 1949 [cited 2021 Aug 14];Available from: https://hdl.handle.net/10217/195976.
24. Heywood H. Numerical definitions of particle size and shape. Journal of the Society of Chemical Industry [Internet]. 1937 [cited 2021 Aug 14];56(7):149-54;Available from: https://doi.org/10.1002/jctb.5000560702.
25. Riley NA. Projection sphericity. Journal of Sedimentary Research [Internet]. 1941 [cited 2021 Aug 14];11(2):94-5;Available from: https://doi.org/10.1306/D426910C-2B26-11D7-8648000102C1865D.
26. Porter A, Lyons BP, Galloway TS, Lewis CN. The role of marine snows in microplastic fate and bioavailability. Environ Sci Technol [Internet]. 2018 [cited 2021 Aug 14];52:7111-9;Available from: https://doi.org/10.1021/acs.est.8b01000.
27. Mani T, Blarer P, Storck FR, Pittroff M, Wernicke T, Burkhardt-Holm P. Repeated detection of polystyrene microbeads in the Lower Rhine River. Environmental Pollution [Internet]. 2019 Feb [cited 2021 Aug 14];245;Available from: https://doi.org/10.1016/j.envpol.2018.11.036.
28. Nguyen TH, Tang FHM, Maggi F. Sinking of microbial-associated microplastics in natural waters. PLOS ONE [Internet]. 2020 Feb 3 [cited 2021 Aug 14];15(2);Available from: https://doi.org/10.1371/journal.pone.0228209.

Tạp chí Phát triển Khoa học và Công nghệ – Engineering and Technology, 4(4):1219-1228

Open Access Full Text Article

Bài nghiên cứu

Đặc trưng lắng đọng của vi nhựa Polystyrene có hình dạng kỳ dị

Nguyễn Thu Hà*

Use your smartphone to scan this QR code and download this article

TÓM TẮT

Vi nhựa là chất ô nhiễm rắn mới xuất hiện trong những năm gần đây nhưng có thể gây hại hệ sinh thái dưới nước bằng cách mang các chất phụ gia độc hại vào mạng lưới thức ăn. Vi nhựa đã được phát hiện dày đặc ở nhiều môi trường nước trên toàn cầu, bao gồm cả sông Sài Gòn, Việt Nam. Việc hiểu rõ về các đặc trưng lắng đọng của vi nhựa có thể giúp dự báo sự lan truyền và góp phần loại bỏ chất ô nhiễm này trong nước. Cho đến nay, động lực học của vi nhựa hầu như vẫn được giả định tương tự như động lực học của bùn cát lơ lửng. Tuy nhiên, vi nhựa có nhiều đặc tính nhân tạo có thể khiến chúng di chuyển khác biệt trong nước so với bùn cát lơ lửng như khối lượng riêng, kết cấu hạt, hình dạng và đặc tính bề mặt. Do đó, nghiên cứu này hướng đến việc điều tra mối tương quan giữa kích thước và hình dạng bất thường của vi nhựa polystyrene với chuyển động thẳng đứng của nó. Thí nghiệm sử dụng phương pháp Particle Tracking Velocimetry (PTV) và thuật toán xử lý hình ảnh tự động để đo đồng thời các đặc tính hình học của vi nhựa và vận tốc lắng trong khi chúng đang lắng tự do trong một cột nước tĩnh. Chúng tôi nhận thấy rằng đường kính hình tròn ngoại tiếp hạt vi nhựa là thông số hình học thích hợp nhất để biểu thị kích thước vi nhựa. Tốc độ lắng của vi nhựa polystyrene có hình dạng kì dị có kích thước từ 0,2 đến 0,9 mm chủ yếu nằm trong khoảng từ 0,5 đến 2,0 mm/s, bằng một nửa của hạt bùn cát nhưng gấp bốn lần so với các hạt keo sinh học có cùng kích thước. Vận tốc lắng tăng gấp hai lần khi kích thước vi nhựa tăng từ 0,2 đến 0,9 mm. Sự gia tăng tính kì dị về hình dạng có thể làm chậm tốc độ lắng của vi nhựa lớn nhưng không ảnh hưởng đến chuyển động thẳng đứng của vi nhựa nhỏ hơn 0,32 mm. Tỷ lệ giữa diện tích hình chiếu vi nhựa và diện tích của hình tròn ngoại tiếp nhỏ nhất được coi là hệ số hình dạng hai chiều của các hạt vi nhựa ba chiều phù hợp nhất để thể hiện mối tương quan giữa kích thước và vận tốc lắng. Do đó, các phương trình tương quan giữa vận tốc lắng và kích thước vi nhựa được đề xuất ở đây có thể được sử dụng như một công cụ đơn giản để ước tính vận tốc lắng của vi nhựa polystyrene có hình dạng bất thường được tìm thấy trong nhiều đề tài lấy mẫu vi nhựa trong môi trường nước tự nhiên.

Từ khoá: vi nhựa, vận tốc lắng/độ thô thủy lực, sự kì dị, hệ số hình dạng, polystyrene

Khoa Kỹ thuật Xây dựng, Trường Đại học Bách Khoa, Đại học Quốc gia Thành phố Hồ Chí Minh, Việt Nam.

Liên hệ

Nguyễn Thu Hà, Khoa Kỹ thuật Xây dựng, Trường Đại học Bách Khoa, Đại học Quốc gia Thành phố Hồ Chí Minh, Việt Nam.

Email: thuhatnn@hcmut.edu.vn

Lịch sử

- Ngày nhận: 14-8-2021
- Ngày chấp nhận: 27-11-2021
- Ngày đăng: 25-12-2021

DOI : 10.32508/stdjet.v4i4.905

Check for updates

VNU-HCM Press

Trích dẫn bài báo này: Hà N T. **Đặc trưng lắng đọng của vi nhựa Polystyrene có hình dạng kỳ dị**. *Sci. Tech. Dev. J. - Eng. Tech.;* 4(4):1219-1228.